Visualization of upward mixed-convection flows in vertical pipes using a thin semitransparent gold-film heater and dye injection

M. A. Bernier
Département de génie mécanique, Ecole Polytechnique de Montréal, Montréal, Québec, Canada

B. R. Baliga
Department of Mechanical Engineering, McGill University, Montréal, Québec, Canada

An experimental technique has been developed to visualize water flows in pipes subjected to a uniform wall heat flux (UHF). The technique is based on the use of a thin semitransparent gold-film heater, glued inside a Plexiglas pipe, and dye injection. The capabilities of this technique were used to examine upward mixed-convection flows in vertical pipes. Most of the earlier experimental studies of the UHF boundary condition employed an opaque heating tube. In contrast, the present technique allows direct visualization of fluid-flow phenomena, such as recirculation cells and laminar-turbulent transition, over the entire length of the heated pipe. Flow visualization and numerical results pertaining to one recirculation cell, for values of $Re = 90$, $Gr_q = 0.33 \times 10^6$ ($Gr_q/Re^2 = 40.7$), and $Pr = 5.6$, are presented in this paper, and the agreement between these results is shown to be qualitatively quite good. Two cases of laminar-turbulent transition are reported in this paper, one for values of $Re = 72$, $Gr_q = 0.7 \times 10^5$, and $Pr = 6.0$; and the other for $Re = 48$, $Gr_q = 0.95 \times 10^5$, and $Pr = 6.0$. It appears as if this is the first presentation of such results for a UHF boundary condition.

Keywords: mixed-convection; flow visualization; recirculation cells; laminar-turbulent transition; gold-film heater

Introduction

An experimental technique for the visualization of mixed-convection flows of water in pipes is described in this paper. The development and testing of this technique was undertaken as part of a complementary numerical and experimental study of closed-loop thermosyphons (Bernier, 1991; Bernier and Baliga, 1992a). The technique is based on the use of a thin semitransparent gold-film heater, glued on the inside surface of a Plexiglas pipe, and dye injection.

In order to ascertain the capabilities of this technique, flow visualization studies were undertaken to obtain qualitative information on two phenomena that can occur in upward mixed-convection flows in vertical pipes subjected to a uniform heat flux (UHF) boundary condition. The first phenomenon pertains to recirculation cells. The start of these cells has been numerically predicted in the past by Lawrence and Chato (1966), but the prediction and behavior of the entire recirculation region have not yet been reported. Furthermore, these cells have apparently never been visually observed. This is because previous experiments, such as the one by Hallman (1958), relied on ohmic heating of opaque walls. The second phenomenon of interest involves the laminar-turbulent transition. Studies by Hallman (1958) and Scheele *et al.* (1960, 1962) have revealed that such transitional flows can exist in upward mixed-convection flows, even when the Reynolds number is well below 2,000. In those studies, however, laminar-turbulent transitions were inferred indirectly from temperature fluctuations recorded by thermocouples (Hallman, 1958; Scheele and Hanratty, 1962) or by flow visualization at the end of an opaque heated tube (Scheele *et al.*, 1960).

A number of researchers have recognized the attraction of the electrically heated thin gold film as a transparent source of uniform heat flux. Baughn *et al.* (1985) used the same type of gold film as the one used in this study to obtain local heat transfer coefficients for various forced convection test problems involving the flow of air. Hippensteele *et al.* (1983, 1985) used a thin transparent gold-film and liquid crystal composite to obtain qualitative and quantitative results of local heat transfer coefficients on a gas turbine blade. In a study undertaken in the Heat Transfer Laboratory at McGill University, Neill (1989) examined the gold-film technique in the context of laminar natural convection along a vertical flat plate and in a horizontal concentric annulus. Neill (1989) also obtained qualitative surface temperature visualization results using the thin gold-film technique in conjunction with liquid crystals.

Address reprint requests to Dr. Bernier at the Département de génie mécanique, Ecole Polytechnique de Montréal, Case postale 6079, succursale A, Montréal, Québec, Canada H3C 3A7.

Received 18 June 1991; accepted 9 December 1991

As reported in these studies, the thin gold-film technique provides a relatively simple and accurate method for determining local heat transfer coefficients and obtaining qualitative surface temperature visualization data for flows ranging from turbulent forced convection to laminar natural convection. However, the studies were performed with air and do not appear to have exploited the transparency of the thin gold film for visualizing internal flows.

In this work, the gold-film technique is used to study upward mixed-convection flows of water inside vertical pipes. Due to constraints imposed by the design of the related closed-loop thermosyphon apparatus of Bernier (1991), the internal diameter of the pipe was fixed at 19 mm, and the gold film had to be attached on the interior surface of the pipe in order to minimize axial wall conduction. Thus, the techniques devised by Neill (1989) to fix the gold film on the exterior surface of a test object, and by Baughn *et al.* (1985) to attach the film to the internal surface of a relatively large diameter (9.5 cm) pipe, could not be used. Therefore, a new construction procedure was needed and is briefly described.

Design and construction of the gold-film sections

Introduction

The thin semitransparent gold film used in this study is commercially available in flat sheets of various sizes, thicknesses, and resistances. It is manufactured by the Sierracin Corporation (Sylmar, CA) under the brand name Intrex. It consists of a thin transparent polyester film on which a coat of gold is applied by means of vacuum deposition. The gold layer is overcoated with a proprietary ceramic coating to protect the gold from abrasion. The main characteristics of the film used in this study are the following: overall thickness of 0.13 mm (0.005 inches); a gold coating thickness estimated at approximately 20 angstroms; maximum sustained operating temperature of 100°C at the coating interface; transparency to light of 80 ± 10 percent; electrical resistivity of 13.54 Ω/sq ± 6.2 percent, as measured by Neill (1989); and a thermal conductivity of the polyester film of 0.28 W/m·K, as reported by Maeda (1989).

The integrity of this type of gold film when bent to a radius of curvature of 9.5 mm, such as the one used in this study, was a major concern at the initiation of this project. Therefore, initial tests were performed to measure the variation in electrical resistance of a gold film bent to such a small radius of curvature. The results of these tests indicated that the change in resistance due to bending was of the order of ± 1 percent (Bernier, 1991). Therefore, bending effects were considered to be negligible.

Construction procedures

A total of four gold-film test sections were built for this study. Two sections were instrumented with thermocouples and two sections were free from thermocouples. The final design and construction procedures for the gold-film test sections evolved over several preliminary efforts. In an early prototype, the polyester side of the film was glued to the inner surface of a Plexiglas pipe. Thus, in this arrangement, the gold surface of the film was in direct contact with the fluid. When this prototype was energized and water was allowed to flow through the pipe, it was found that the electrical resistance of the gold film almost doubled over 1 hour, indicating that it was deteriorating rapidly. This problem is believed to be due to erosion and/or corrosion processes, as a visual inspection of the gold film at the end of this test indicated that patches of gold had been removed from the film. Based on this experience, it was decided to protect the gold coating by gluing the gold side of the film to the Plexiglas pipe, thus leaving the polyester side of the film in contact with the water. The disadvantage of this latter technique is that, unlike the case where the gold coating is touching the fluid, there is a thermal resistance between the gold coating and the fluid, due to the presence of the polyester film (0.13 mm thick).

The final gold-film test section was built using two half-sections of the Plexiglas pipe. This so-called split design consisted of several steps that are briefly described in the next paragraphs. Cross-sectional views of a completed gold-film test section are presented in Figure 1.

Cutting, painting, bending, and gluing of the gold film

Plexiglas pipes with an internal diameter of 19.05 mm and an external diameter of 25.4 mm were cut in the longitudinal direction to obtain half-sections of an outer radius of 12.7 mm. As indicated in Section A-A in Figure 1, a groove was cut in the longitudinal flat edge of one of the two half-sections to accommodate a sealing gasket.

The gold film used in this study is very fragile, thus the procedures described in this section had to be undertaken with

Notation

C_p Specific heat at constant pressure
D Internal diameter of the test section
Gr_q Grashof number based on heat flux $\left[\frac{g\beta q D^4}{\nu^2 k_f}\right]$
g Acceleration due to gravity
k_f Thermal conductivity of the fluid
L Length of the heated portion of the gold-film test section
P_w Power input to the gold-film test section
Pe Péclet number (Re·Pr)
Pr Prandtl number ($\mu C_p/k_f$)
q Heat flux at the inner surface of the gold-film test section ($P_w/\pi DL$)
Re Reynolds number ($\rho VD/\mu$)
T Temperature
T_a Ambient temperature
T_o Inlet temperature to the test section
T_w Inner surface wall temperatures in the heated section
u, v Axial and radial velocity components, respectively
V Average velocity at the inlet of the test section
z Axial coordinate

Greek symbols

β Thermal volumetric expansion coefficient
μ Dynamic viscosity
ν Kinematic viscosity
ρ Density of the fluid
ψ Dimensional stream function

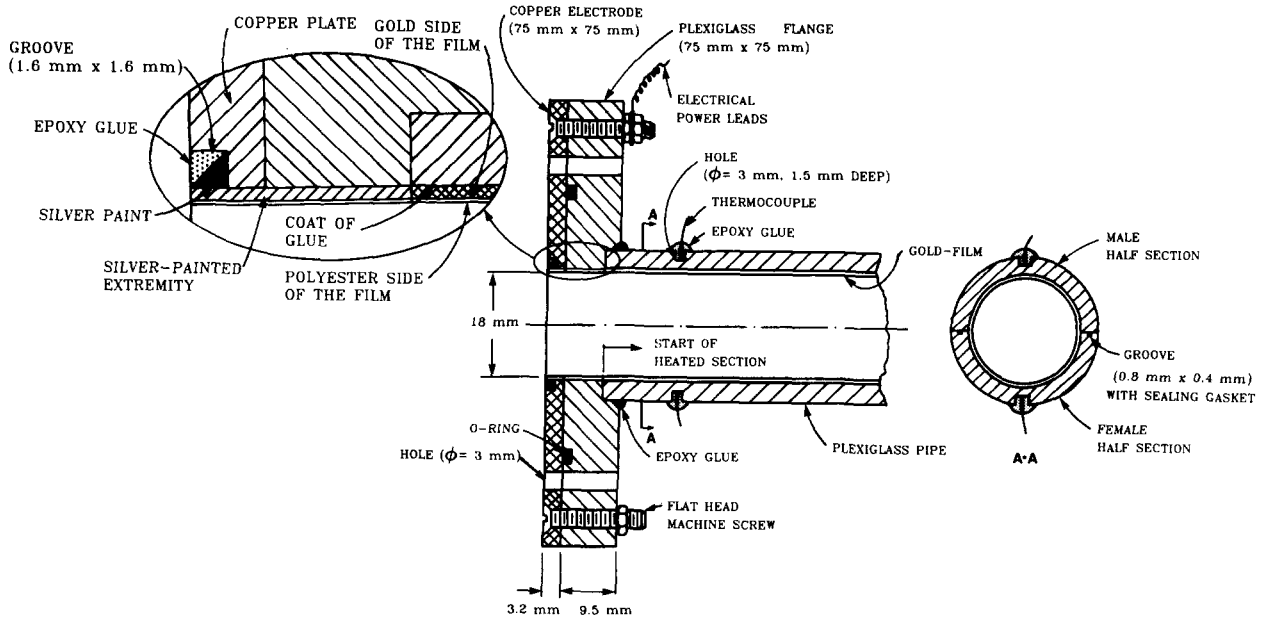

Figure 1 Cross-sectional views of a gold-film flow visualization section

great care. Both sides of the gold film were covered with removable transparent tape (3M, Scotch Brand MagicPlus) to protect the film, and, as an extra protection, the gold film was always handled with clean surgical gloves.

Gold-film strips were first cut from a large sample roll. These strips were cut wider than the half internal circumference of the Plexiglas pipe. The excess width was cut off at a later stage of construction, after the film was firmly attached to the surface of the Plexiglas pipe. Both extremities of each strip were then painted with a silver-loaded paint (Sunshine Scientific Instruments, Part No. C-24) to provide electrical contact between the gold film and copper electrodes (Figure 1). Attachment of the gold film to the inner surface of the Plexiglas was achieved by using a two-part epoxy glue (Devcon, 2-Ton Clear Epoxy). The epoxy glue was poured on the gold side of the strip and once the strip was fully wetted by the glue, it was inserted into the half-section of Plexiglas pipe. Then a specially machined brass rod was used to press it against the pipe half-section.

Mating and sealing of the two half-sections

In order to form a complete gold-film test section, the two Plexiglas half-sections had to be assembled and sealed together. Since the two half-sections were electrically connected in parallel, the values of the electrical resistances of both half-sections had to be very close to ensure that the electric current would be the same in both half-sections, e.g., the half-sections of the flow visualization section used in this work had values of electrical resistances equal to 311 and 310 Ω. The assembly was started by inserting a sealing gasket in the grooved half-section and carefully aligning the two half-sections. Then, approximately 20 hose clamps were used to squeeze these two half-sections together until the external diameter of the newly formed pipe was within ±0.08 mm of the original 25.4 mm external diameter of the Plexiglas pipe. A few drops of Krazy Glue were then applied along the entire length of both seams. This mating and sealing technique provided a good leak-proof seal for the range of pressures encountered in this work (2–3 m of water).

Electrode construction

Details of the final electrode design can be seen in Figure 1. Square copper plates (75 × 75 mm), with a thickness of 3.2 mm and a central hole with a 19 mm diameter, were used as electrodes to connect both extremities of the gold film to the external power leads. Each copper plate was tightly screwed against a Plexiglas flange, with four flat-head stainless-steel machine screws. These assemblies were then carefully inserted over the ends of the gold-film section until, at each end, the silver-painted extremity of the gold film was flush with the external surface of the copper plate. A permanent electrical connection was achieved by joining the copper plates to the silver-painted extremities of the gold film with three coats of silver-loaded paint. This paint was applied along a specially machined groove around the circumference of the central hole in the copper plate. The three coats of paint are represented by a dark triangle in the insert of Figure 1. The remaining space in the groove was then filled with epoxy glue so as to seal the paint from the outside environment.

At this stage, the construction of the gold-film section is complete. The nominal internal diameter of the four gold-film sections, D, was measured and found to be equal to 18 mm. Considering that the film is 0.13 mm thick, the thickness of the glue is then approximately equal to 0.40 mm. The length of the heated portion of each gold-film section, L, was equal to 0.664 m. The electrical resistances of the various gold-film sections were monitored during construction. These resistance values are presented in the work of Bernier (1991), where it is shown that the various construction procedures described earlier, from the initial cutting stages to the final electrode assembly, did not affect the integrity of the gold film.

Gluing of thermocouples in the heated sections

Holes were drilled through the Plexiglas pipe to accommodate thermocouples in two of the gold-film test sections, as shown in section A-A in Figure 1. A total of 46 chromel-constantan (type E) thermocouples, 23 in each half-section, were glued into these holes in order to measure wall temperatures. These

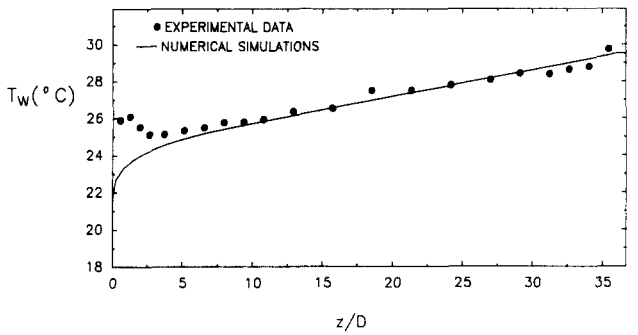

Figure 2 Axial variation of wall temperatures in the heated section: Comparison between experimental data and numerical simulations for Pr = 6.3, Re = 140, and $Gr_q = 0.49 \times 10^6$

heated sections were then insulated with 6 cm of foamed-plastic insulation ($k = 0.04$ W/m·K). The holes had a diameter of 3.0 mm and a depth of 1.6 mm, half the thickness of the wall of the Plexiglas pipe. With this arrangement, the thermocouples were approximately 2.13 mm away from the inner surface. This included 0.13 mm (thickness of the polyester portion of the film) from the inner surface to the gold coating, 0.40 mm (glue) from the gold coating to the inside surface of the Plexiglas pipe, and 1.6 mm from the inside surface of the Plexiglas pipe to the thermocouples. Thus, to obtain the true inner surface temperatures, the measured temperatures had to be corrected. The correction procedure, which has been discussed by Bernier (1991), is based on the assumption of locally one-dimensional radial heat conduction in the pipe wall and the film. Since the thermal resistance from the gold coating to the inner surface was much smaller than the thermal resistance from the gold coating to the ambient, the value of the temperature correction was essentially equal to the temperature drop from the gold coating to the inner surface. The temperature from the gold coating to the thermocouples was essentially uniform. For the results presented in Figure 2, which will be discussed shortly, the value of the temperature correction was of the order of −0.5°C.

Supporting equipment and experimental procedures

Fluid flow circuit

The fluid flow circuit is shown schematically in Figure 3. The flow circuit employed in this study used all the components of the closed-loop thermosyphon of Bernier (1991), except that the cooled section was removed and replaced by flexible pipes that were connected to a temperature-controlled constant-head tank and to a flow diverter. In this arrangement, distilled water flows by gravity into the loop from the constant-head tank. After travelling around the loop, the water is fed to a flow diverter. Then, the water flows either into a bucket, when an overall flow rate measurement is performed, or back to a constant-temperature bath. The stability of the flow rate using this setup was observed to be better than ±1 percent (Bernier, 1991).

Water was pumped from a temperature-controlled water bath (Neslab, model RTE-220A) to the bottom of the constant-head tank. Then, the water moved upward in the tank and overflowed into the inner tank to finally return to the constant-temperature bath. With this setup, the temperature of the water in the constant-head tank could be maintained constant to within ±0.05°C. In the flow visualization experiments, the bath temperature was set such that the inlet temperature to the flow visualization section was within ±1 C of the ambient temperature. This minimized heat losses (or gains) from the flow visualization section.

Flow rate, temperature, and power measurements

The mass flow rate in the fluid flow circuit was obtained by measuring the mass of water that accumulated in a bucket over a fixed time interval measured by a stopwatch (International Standard Organization, 1980). The uncertainty associated with this mass flow rate measurement was estimated to be ±1 percent (Bernier, 1991). When needed, the average velocity at the inlet of the heated section, V, was determined from a knowledge of the cross-sectional area of the pipe and the density of water.

Pipe wall temperatures in the heated section and the ambient fluid temperature were measured using chromel-constantan (type E) thermocouples. These thermocouples were carefully calibrated against a quartz thermometer. A microprocessor-based data acquisition and control system (Hewlett-Packard model HP3497A) was used to measure the voltage output of these thermocouples, convert them to temperature readings, and record these readings. The uncertainty associated with these thermocouple measurements was estimated by Bernier (1991) to be ±0.05°C.

Electrical power was provided to the test section by a DC power supply (Sorensen, model DCR300-3B). The actual power input, P_w, was obtained from current and voltage measurements. Current was measured using a multimeter (Hewlett-Packard, model HP3478A). Voltage measurements across the gold-film sections were obtained using a separate multimeter (Keithley, model 195A). The uncertainty in the P_w measurement was estimated at less than ±0.5 percent (Bernier, 1991).

Dye injection technique

As reported by Macagno (1969), a number of methods are available for flow visualization in liquids. The most prominent

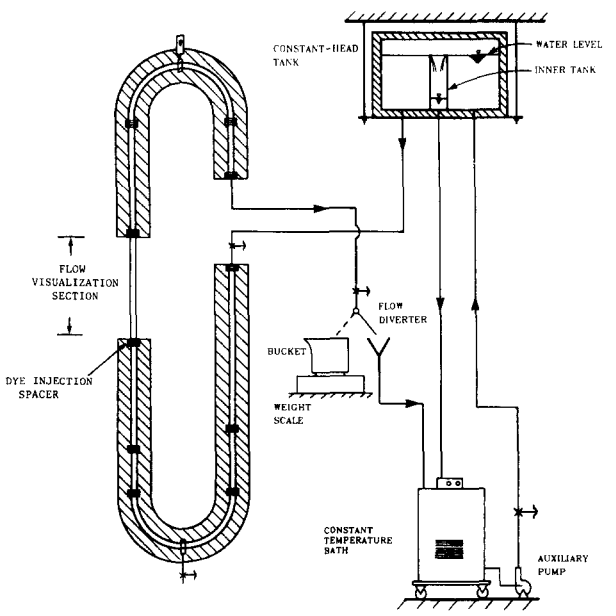

Figure 3 Schematic of the fluid flow circuit

ones are (1) the hydrogen-bubble method (Mueller, 1983); (2) injection of small particles, such as aluminum powder (Morton *et al.*, 1989); (3) pH indicator technique (Baker, 1966; Sparrow *et al.*, 1984); and (4) dye injection (Merzkirch, 1974).

In the present study, the dye injection method was used to visualize the flow because of past experiences with the technique in the Heat Transfer Laboratory at McGill University. Another advantage of the dye injection method was that the same setup could be used to study recirculation cells and the laminar-turbulent transition.

The flow was best visualized by injecting a fluorescent dye (fluorescein sodium salt, Sargent-Welch no. SC12184). Nonfluorescent dyes, such as milk and food colorants, were tried, but they did not provide the same degree of contrast that was obtained with the fluorescent dye. The fluorescent dye also had a small molecular diffusion rate, which made it well suited for visualization of fluid pathlines. The dye was prepared by completely dissolving approximately 2 g of dye powder with 1 L of distilled water. At this level of dilution, the dye solution was essentially neutrally buoyant with respect to the water in the flow circuit.

The key elements of the dye injection setup consisted of a small injection tube, an air-pressurized dye reservoir, and illuminating lights. The dye injection tube was made of brass and was part of a special spacer that was inserted immediately upstream of the inlet of the flow visualization section, as shown in Figure 3. The internal and external diameters of the brass injection tube were 0.8 and 1.6 mm, respectively, and the tube was 25 mm long in the flow direction. This injection tube was bent at a 90° angle and positioned at the geometric center of the pipe with the injecting leg parallel to the flow. The length and diameter of the brass tube were such that, when needed, a relatively large volume of dye could be provided at the same local inlet temperature as that of the water flowing in the flow visualization section, without significantly disturbing the main flow. The brass tube was linked to a 200 cm^3 reservoir, which was filled with 80 cm^3 of dye and air pressurized up to 0.4 MPa. A valve located at the outlet of the reservoir permitted regulation of the dye flow rate from a trickle to a flooding condition.

During the flow visualization tests, the dye was illuminated using two 15 W long-wave black lights (Panasonic Blacklight Blue F15 T8/BL-B) positioned on each side of the flow visualization section. The best photographic results were obtained when the rest of the laboratory was in total darkness and a black felt cloth was placed behind the flow visualization section. A number of different photographic films were tried. The best photographs were obtained using either an Agfachrome slide film (ASA 1,000, with a typical camera setting of 1/30 s and f1.8) or a Kodacolor Gold color print film (ASA 400, 1/15 s and f1.8).

For the observations of recirculation cells (Figure 4), the water flowing in the flow visualization section was flooded with the dye, using a method similar to the one described by Scheele and Hanratty (1962). This technique consisted of injecting a large quantity of dye for a short period of time (typically 1 s). A portion of this dye gets trapped in the recirculation cell and stays in the test section for a longer period than the rest of the dye, which gets washed away with the water flowing out of the test section. This process would typically take about 10 minutes before the contours of the recirculation cell became clearly visible and could be photographed. The dye trapped in the recirculating cell would eventually disappear due to molecular diffusion of the dye.

Transitional flows, such as the one shown in Figure 5a, were observed by injecting a continuous filament of dye at the inlet of the flow visualization section. The injection of a dye filament, in a flow where natural convection effects are important, is at best difficult. The difficulties lie in matching the temperature and velocity of the dye, respectively, with the temperature and the relatively small velocity of the main flow. The temperature of the dye has to be equal to that of the primary fluid at the exit of the injection tube, otherwise the dye sinks down or rises abnormally. This requirement was satisfied by letting the dye sit in the brass tube for at least 10 minutes before each injection. As for the flow rate of the injected dye, it has to be high enough to produce a visible and continuous dye filament and low enough to minimize disturbances to the main flow. This could only be achieved by a trial and error procedure. The second observation of a laminar-turbulent transition flow reported in this paper, which is presented in Figure 5b, was obtained by flooding the flow field with dye in a manner similar to the one used to observe recirculation cells.

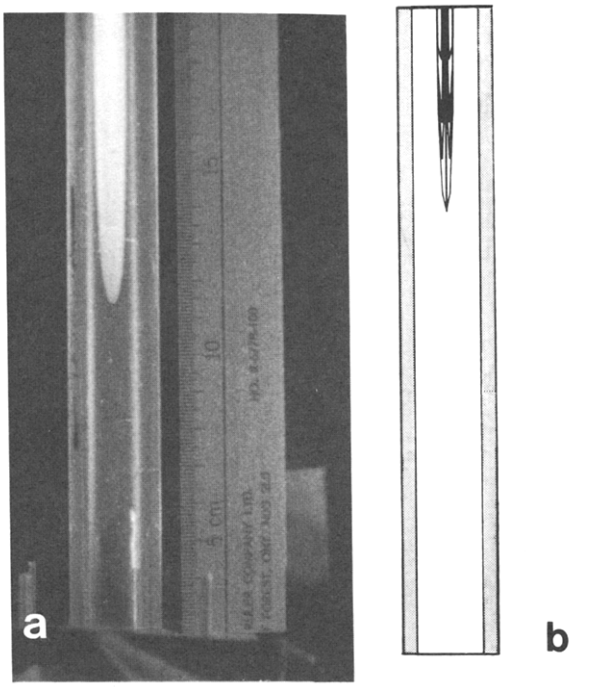

Figure 4 Recirculation cell in a mixed-convection flow for Re = 90, $Gr_q = 0.33 \times 10^6$, Pr = 5.6: (a) flow visualization experiments; (b) corresponding numerical streamlines

Numerical simulations

Numerical simulations were undertaken in conjunction with the experimental investigation. The problem of interest is one of conjugate heat conduction and two-dimensional axisymmetric laminar mixed-convection in vertical pipes subjected to a uniform heat flux boundary condition. The problem is governed by the Navier-Stokes equations, the continuity equation, and the energy equation, all in cylindrical coordinates. Since it was anticipated that recirculation cells would occur, the elliptic versions of the governing equations were used. The finite-volume method of Patankar (1980) and the SIMPLEC algorithm of Van Doormaal and Raithby (1984) were employed to numerically solve these equations. The complete details on the formulation, implementation, and testing of the numerical method can be found in the work of Bernier (1991) and Bernier and Baliga (1992b); therefore, only a succinct description is presented below.

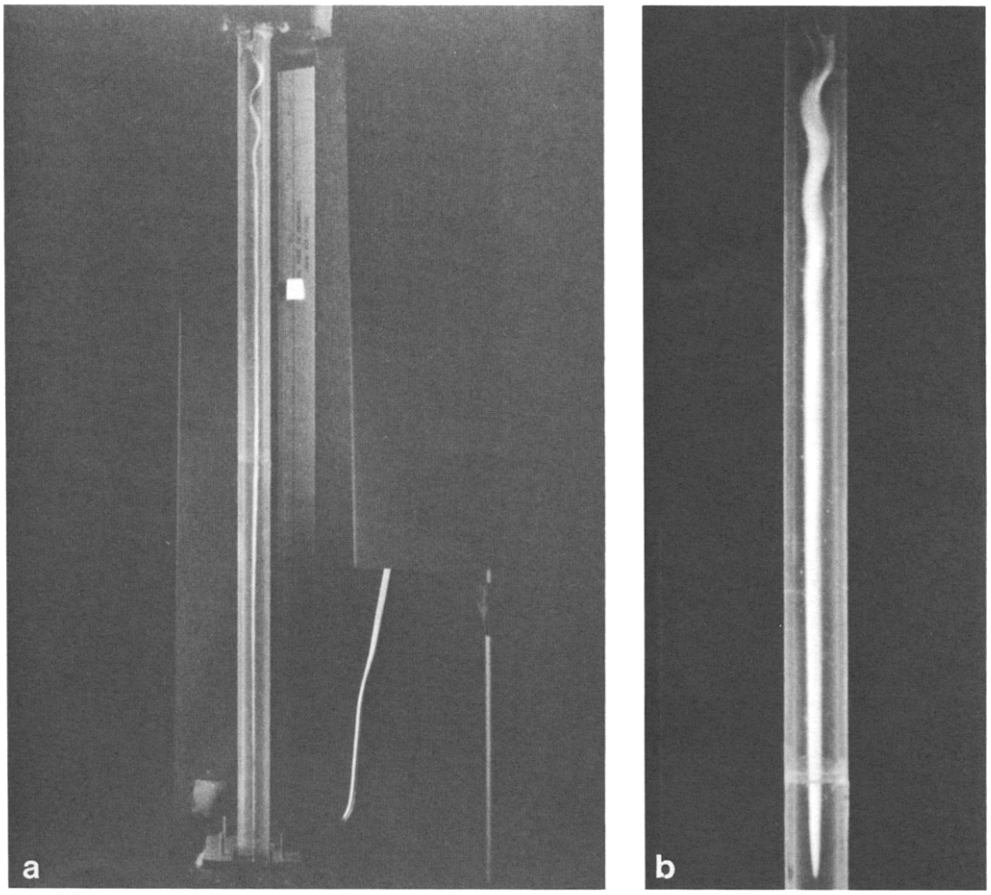

Figure 5 Observations of laminar-turbulent transition in mixed-convection flows: (a) Pr = 6.0, Re = 72, and $Gr_q = 0.7 \times 10^5$; and (b) Pr = 6.0, Re = 48, and $Gr_q = 0.95 \times 10^5$

In experiments such as the one undertaken in this work, it is seldom possible to achieve a strict UHF boundary condition directly at the solid–fluid interface. In most cases, the heat flux is either applied on the exterior surface of a pipe or provided by ohmic heating of the pipe wall. In both cases, the heat flux could be redistributed upstream and downstream of the heated portion of the test section by heat conduction in the wall. As pointed out by Bernier and Baliga (1992b) for the case of the externally applied heat flux, this heat flux redistribution becomes significant when the Péclet number is small, the solid-to-fluid thermal conductivity ratio is high, and/or the thickness to pipe diameter ratio is high. In the present case, the very thin gold coating supplies the heat flux, and it is located between the 0.13-mm thick polyester film and the inside surface of the Plexiglas pipe. In this arrangement and with the relatively high Pe encountered in this study, Bernier (1991) has shown that the heat flux redistribution is negligible. Therefore, under these circumstances, the governing parameters are the Grashof number, Gr_q, the Prandtl number, Pr, and the Reynolds number, Re.

In the numerical simulations, the length of the calculation domain was 1 m ($L/D = 55$). This included a 0.05 m long section upstream of the heated section, 0.664 m for the heated section, and a 0.286 m long section downstream of the heated section. In the radial direction, the calculation domain extended from the pipe centerline to the outer surface of the Plexiglas pipe.

The following boundary conditions were used at the inlet plane of the calculation domain: the axial component of the velocity in the fluid region was specified using the Poiseuille parabola, and the radial velocity component was set equal to zero; both of these velocity components were set equal to zero in the solid region. The portion of the inlet plane in the solid region was assumed to be adiabatic.

At the outlet plane, it was assumed that the axial component of the velocity was positive over the entire fluid region (strictly outflow), and it was assumed that $\partial u/\partial z = 0$, $\partial T/\partial z = 0$, and $v = 0$. In the solid region, the outlet boundary was assumed to be adiabatic, and the velocity components were set equal to zero. Preliminary numerical tests showed that with the outlet plane located 0.286 m downstream of the heated section, this outflow boundary treatment had no perceptible influence on the fluid flow and heat transfer results over most of the length of the calculation domain (Bernier, 1991).

At the outer surface of the Plexiglas pipe, an adiabatic condition was assumed. This last assumption was good considering that (1) the temperature of the water entering the test section was within 1°C of the ambient air temperature in the laboratory, and (2) the Plexiglas pipe has a relatively low value of thermal conductivity (≈ 0.19 W/m·K). In the Plexiglas and gold-film regions of the calculation domain, the viscosity was set equal to a very large value ($\approx 10^{30}$ kg/m·s). At each grid point in the fluid region, suitable temperature-dependent viscosity and thermal conductivity values were prescribed (Weast and Lide, 1989) at the start of each overall iteration of the SIMPLEC solution procedure. The Boussinesq approximation was used to handle the variation of density in the fluid regions. The harmonic-mean practice of Patankar

(1978) was used to obtain the values of viscosity and thermal conductivity at the control volume faces.

The type-B grid of Patankar (1980) was used to discretize the calculation domain. In the fluid, 100 and 20 grid points were used in the axial and radial directions, respectively. In the Plexiglas pipe and in the gold film, the axial distribution of grid points was the same as in the fluid, and 7 grid points were employed in the radial direction. Preliminary numerical tests (Bernier, 1991) showed that this grid gave essentially grid-independent results. In the gold film, a uniform volumetric heat generation term was specified.

Visualization results for upward mixed-convection flows

Recirculation cells

During the course of this study, recirculation cells were experimentally observed for a number of cases representative of mixed-convection situations. A photograph of one such case is presented in Figure 4a. It corresponds to the following conditions: $V = 0.417$ cm/s, $P_w = 19.43$ W, $T_0 = 25.6$°C, and $T_a = 26.3$°C. The corresponding nondimensional parameters were evaluated at the mean fluid temperature in the flow visualization section, and for this particular case they are Re = 90; $Gr_q = 0.33 \times 10^6$ ($Gr_q/Re^2 = 40.7$); and Pr = 5.6. These variables and nondimensional parameters are described in the Notation.

The mixed-convection flow presented in Figure 4a was also investigated numerically. Streamline plots obtained from the numerical simulations are presented in Figures 4b and 6. In Figure 4b, only the first one-third of the flow visualization section is shown, so as to correspond with the experimental results presented in Figure 4a. Streamlines over the fluid region of the calculation domain are presented in Figure 6 where, for reasons of clarity, the scale in the radial direction has been drawn to 10 times the scale in the z-direction. In Figure 6, at about the mid-height location, starting from the pipe wall and going toward the centerline, the streamlines plotted are $\psi/\psi_{max} = 0.91$, 0.79, 0.67, 0.55, 0.43, 0.30, 0.18, 0.12, 0.061, 0.030, 0.0061, 0, −0.0030, −0.0024, −0.0018, −0.0012, and −0.0060, where ψ_{max} corresponds to the maximum value of the stream function in the calculation domain. In Figure 4b, only the streamlines encompassing the recirculation cell have been plotted. As is quite evident from Figure 6, the recirculation region terminates well before the outlet plane. Thus, the aforementioned requirement that the outlet plane be a strict outflow boundary is comfortably satisfied.

Recirculation cells have been predicted numerically and observed experimentally by Morton *et al.* (1989) for mixed-convection flows of water in vertical pipes for uniform wall temperature cases. However, for a uniform heat flux boundary condition, these cells have apparently never been numerically predicted past the start of the cell. For example, Lawrence and Chato (1966) predicted the onset of flow reversals, but because their investigation was conducted with a parabolic numerical method, it was not possible to study the entire flow reversal region. Furthermore, flow reversals in vertical pipes subjected to a uniform heat flux boundary condition have not yet been observed experimentally, because the uniform wall heat flux boundary condition is usually provided by an opaque electrically heated pipe (Hallman, 1958), thus precluding any flow visualization studies.

Physically, the existence of these recirculation cells can be explained as follows. Due to the relatively large value of Pe (= 504) in this case, and the absence of any significant axial

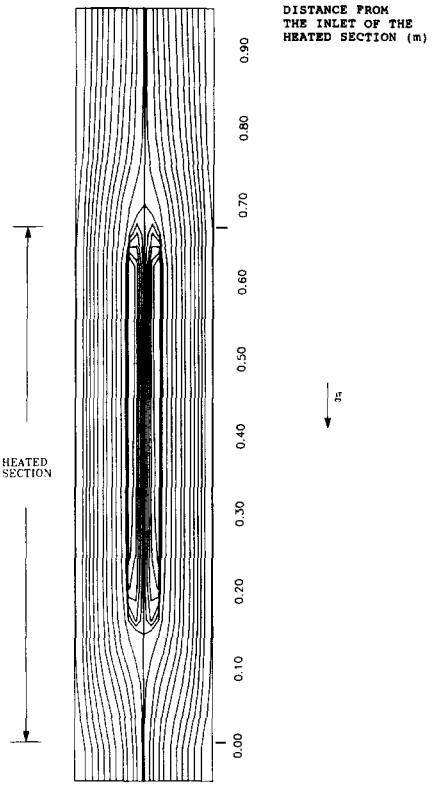

Figure 6 Numerically predicted streamlines in the fluid region of the full calculation domain for Re = 90, $Gr_q = 0.33 \times 10^6$, Pr = 5.6. Note, the scale of the radial direction is 10 times the scale of the axial direction

heat conduction in the pipe wall, the fluid flow is essentially unaffected by the ohmic heating of the gold film until it actually enters the heated section; thus, the fluid enters the heated section with a fully developed parabolic velocity profile and a uniform temperature. In the heated section, the fluid near the wall is heated, and its density becomes lower than that of the fluid further from the wall. This density difference, in conjunction with the gravitational force field, leads to a buoyancy force that causes the fluid to accelerate in the region next to the wall. To satisfy mass conservation, the increase in fluid velocity and associated mass flow rate in the vicinity of the wall is fed by fluid drawn from the pipe centerline region. In turn, this moves the point of maximum axial velocity toward the wall. This also progressively depletes the fluid near the center of the pipe up to a point where the axial velocity at the centerline of the pipe becomes zero and then negative (opposite to the main flow direction). The start of the recirculation cell corresponds to the point where the centerline velocity becomes zero. The location where the cell starts is dependent on the values of the governing parameters. For fixed values of Re and Pr, the start of the cell has been observed to move upstream with an increase in Gr_q. Similar results have been obtained by Lawrence and Chato (1966) for a uniform heat flux boundary condition, but with a uniform inlet velocity profile.

Beyond the start of the recirculation cell, the fluid near the wall continues to accelerate, and to fulfill the mass conservation requirements, the fluid near the centerline of the pipe must flow in the opposite direction to that of the main (or overall) flow. Some distance downstream of the outlet of the heated section, the temperature of the fluid becomes uniform, and its velocity profile reverts to the Poiseuille parabola. This establishes a

closed zone within which the fluid recirculates. In any cross section of this zone, part of the fluid moves in the direction of the main flow and an equal amount of fluid flows in the opposite direction. About 5 cm downstream from the start of the recirculation zone, the streamlines become essentially parallel to one another, indicating that the flow has reached a fully developed condition, where the velocity profile does not change with axial distance. In this fully developed region, the buoyancy, pressure, and viscous forces balance each other. At the exit of the heated section, there is a sudden decrease in the level of buoyancy forces, and the viscous forces, which now dominate, cause the fluid near the wall to decelerate. The excess fluid is directed toward the centerline, where the axial velocity becomes positive. Finally, at the end of the upstream section, the shapes of the streamlines are almost identical to those at the inlet of the calculation domain. This indicates that the parabolic velocity profile has been reestablished at the outlet.

As is seen in Figure 4, the recirculation cell starts at $z \approx 11.5$ cm in the experiment and at $z \approx 14$ cm in the case of the numerical results. Assuming that the numerical simulations are accurate, this difference could be due to three factors. Firstly, near the start of the cell, the axial velocities are very small, so that the dye is advected away very slowly with the main flow. It is, therefore, possible that the apex of the cell shown in Figure 4a represents a zone of very slow upward-moving fluid, and not the exact start of the recirculation zone. However, this phenomenon is not believed to be that significant in this particular example as the observed apex remained stationary for approximately 10 minutes, within the reading accuracy of the ruler (± 1 mm). The second factor is that in the regions of low flow velocity, such as the start of the recirculation cell, there could be some upstream (with respect to the main flow) diffusion of the dye. The third, and perhaps the most significant, factor is believed to be due to the fact that, at the entrance of the flow visualization section, the heat flux was greater than the average value assumed in the numerical simulations. This is discussed further in the following paragraph.

As was stated earlier, two of the gold-film test sections used in this study were equipped with thermocouples to measure wall temperatures. Experiments were performed with these heated sections to measure local variation of wall temperatures (Bernier, 1991). The results of one such experiment are shown in Figure 2, where local variations of wall temperatures, T_w, are plotted against a nondimensional length (z/D), with $z/D = 0$ representing the start of the heated section. For the temperatures encountered in these experiments, Pr = 6.3, the average velocity was 0.7 cm/s (Re = 140), and the power input was 39.8 W ($Gr_q = 0.49 \times 10^6$). The dots shown in Figure 2 represent the experimentally measured values, and the solid line pertains to local wall temperatures predicted by numerical simulations. The numerical results were obtained by assuming constant fluid properties evaluated at the mean fluid temperature in the heated section. As indicated earlier, the uncertainty in the experimentally measured wall temperature was estimated at ± 0.05°C. The uncertainty associated with the axial positioning of the thermocouple was ± 0.5 mm. Both of these uncertainty values are well within the diameter of the dots presented in Figure 2. The agreement between the predictions of the numerical simulations and the experimental measurements is quite good except in the entrance region, $z/D \leqslant 5$, where the measured wall temperatures are higher than the numerical predictions.

It is believed that, under the conditions of thermal expansion and contraction experienced by the gold-film sections, the electrical link between the gold film and the copper electrodes weakened with time, causing a local increase in the value of the electrical resistance at the electrode–gold film interface. This created a greater than average heat flux and higher than normal wall temperatures, as seen in Figure 2, in the vicinity of those locations.

The flow visualization section that was used to obtain the results presented in Figure 4 (and in Figure 5, which will be discussed next) was not equipped with thermocouples, so that the corresponding wall temperatures could not be recorded. However, it is conceivable that this flow visualization section had problems similar to those described above, since all gold-film sections were assembled in the same way. If that were indeed the case, then the fluid was heated with a greater than average heat flux near the inlet. Thus, the buoyancy effects, which are responsible for the initiation of the recirculation cell, would be greater in the experiments than those in the numerical simulations. Therefore, the recirculation zone in the experimental results would start sooner than that in the numerical predictions.

Laminar-turbulent transition

Several cases of laminar-turbulent transitions in mixed-convection flows were observed during the course of the flow visualization studies. Two such cases are presented in Figure 5 for two different dye injection techniques. Transition is defined here as the condition in which an injected dye tracer deviates from its steady streamline motion to a somewhat unsteady wave-like motion. In Figures 5a and b, the operating conditions correspond to Re = 72, $Gr_q = 0.7 \times 10^5$, and Pr = 6.0, and to Re = 48, $Gr_q = 0.95 \times 10^5$, and Pr = 6.0, respectively.

Figure 5a was obtained by injecting a continuous filament of dye at the entrance of the flow visualization section. As can be seen, the injected dye filament becomes unstable. A visual inspection close to the end of the flow visualization section indicated that the instability starts to be apparent approximately 0.47 m from the inlet. This occurrence is indicated by the white marker on the ruler in Figure 5a. Figure 5b was obtained by flooding the flow field with dye in a manner similar to the one used to observe recirculation cells. The results presented in Figure 5b suggest the presence of a recirculation cell. However, careful monitoring of the location of the lower tip of this apparent recirculation region indicated that it was moving upward at a velocity of ≈ 3 mm/min. This was in contrast with the stationary apex of the recirculation cell presented in Figure 4a. Numerical simulations performed for the same nominal set of parameters, as those corresponding to Figure 5b, did not indicate the presence of a recirculation cell.

The results presented in Figure 5 provide further evidence of the existence of laminar-turbulent transition in mixed-convection flows. As was noted in the introduction, Hallman (1958) relied on wall temperature fluctuations to determine laminar-turbulent transition, as he could not observe the flow through his opaque heating tubes. Scheele *et al.* (1960) determined such transitions by observing the behavior of an injected dye filament at the exit of an opaque heating tube. The major advantage of the semitransparent gold-film technique developed for this study is that, unlike the techniques of Hallman (1958) and Scheele *et al.* (1960), the injected dye, and consequently the flow field, can be visualized over the full length of the heated section.

The existence of a transition zone in low Reynolds number ($< 2{,}000$) mixed-convection flows is believed to be due to the presence of inflexion points in the axial velocity profile, which facilitate destabilization of the flow (Scheele and Hanratty, 1962). Numerical simulations confirmed the presence of such inflexion points. For the conditions of Figures 5a and b, the start of inflexion points was numerically predicted at $z/D \approx 4$ and at $z/D \approx 6$, respectively (Bernier, 1991). However, in the experimental results presented in Figures 5a and b, the start of

the transition region occurs at $z/D \approx 26$ and $z/D \approx 28$, respectively. These differences may be due to the fact that disturbances need some distance to grow before they become noticeable, as was noted by Hallman (1958) and Scheele *et al.* (1960).

Concluding remarks

This paper described a technique that allows visualization of water flows in pipes subjected to a uniform wall heat flux. The technique is based on the use of a thin semitransparent gold film and dye injection. Some of the capabilities of this technique have been demonstrated by observing the presence of recirculation cells and laminar-turbulent transitions, which often occur in upward mixed-convection flows of water in vertical pipes. The experimental observation of a recirculation cell was compared with corresponding numerical predictions, and there was good qualitative agreement between these results. It appears as if this is the first presentation of such results.

Most of the earlier experimental studies of upward mixed-convection flows with a UHF boundary condition employed an opaque heating tube. In contrast, the present technique allows direct visualization of fluid-flow phenomena, such as recirculation cells and laminar-turbulent transition, over the entire length of the heated pipe. Thus, the technique developed in this study could be a valuable experimental tool for further studies on mixed-convection flows in pipes.

Acknowledgments

This research was financially supported by the Natural Sciences and Engineering Research Council of Canada, in the form of a Post-Graduate Scholarship granted to M. A. Bernier and through individual operating grants awarded to Professor B. R. Baliga.

References

Baker, D. J. 1966. Technique for the precise measurement of small fluid particles. *J. Fluid Mech.* **26**, 573–575

Baughn, J. W., Takahashi, R. K., Hoffman, M. A. and McKillop, A. A. 1985. Local heat transfer measurements using an electrically heated thin gold-coated plastic sheet. *ASME J. Heat Transfer.* **107**, 953–959

Bernier, M. A. 1991. Investigation of a closed-loop thermosyphon. Ph.D. thesis, McGill University, Montréal, Canada

Bernier, M. A. and Baliga, B. R. 1992a. A 1-D/2-D model and experimental results for a closed-loop thermosyphon with vertical heat transfer sections. *Int. J. Heat Mass Transfer.* in press

Bernier, M. A. and Baliga, B. R. 1992b. Conjugate conduction and laminar mixed-convection in vertical pipes for upward flow and uniform wall heat flux. *Numer. Heat Transfer—Applications.* in press

Hallman, T. H. 1958. Combined forced and free convection in a vertical tube. Ph.D. thesis, Purdue University, West Lafayette, IN, USA

Hippensteele, S. A., Russell, L. M. and Stepka, F. S. 1983. Evaluation of a method for heat transfer measurements and thermal visualization using a composite of a heater element and liquid crystals. *ASME J. Heat Transfer.* **105**, 184–189

Hippensteele, S. A., Russell, L. M. and Torres, F. J. 1985. Local heat-transfer measurements on a large-scale model turbine blade airfoil using a composite of a heater element and liquid crystals. *ASME J. Eng. Gas Turbines Power.* **107**, 953–960

International Standard Organization. 1980. Mesure de débit des liquides dans les conduites fermées—Méthode par pesée. Norme Internationale ISO 4185-1980(F)

Lawrence, W. T. and Chato, J. C. 1966. Heat-transfer effects on the developing laminar flow inside tubes. *ASME J. Heat Transfer.* **88**, 214–222

Macagno, E. O. 1969. Flow visualization in liquids. Iowa Institute of Hydraulic Research, IA, USA, Report No. 114

Maeda, Mr. 1989. Toriay Company, Plastic and film division, personal communication

Merzkirch, W. 1974. *Flow Visualization.* Academic Press, New York

Morton, B., Ingham, D. B., Kenn, D. J. and Heggs, P. J. 1989. Recirculating combined convection in laminar pipe flow. *ASME J. Heat Transfer.* **111**, 106–113

Mueller, T. J. 1983. Hydrodynamic flow visualization. *Fluid Mechanics Measurements* (R. J. Goldstein, Ed.), Hemisphere, Washington, DC

Neill, W. S. 1989. Local natural convection heat transfer measurements using a thin gold-film technique. M.Eng. thesis, McGill University, Montréal, Canada

Patankar, S. V. 1980. *Numerical Heat Transfer and Fluid Flow.* Hemisphere, Washington, DC

Patankar, S. V. 1978. A numerical method for conduction in composite materials, flow in irregular geometries and conjugate heat transfer. *6th Int. Heat Transfer Conf.* **3**, 297–302

Scheele, G. F., Rosen, E. M. and Hanratty, T. J. 1960. Effect of natural convection on transition to turbulence in vertical pipes. *Can. J. Chem. Eng.* **38**, 67–73

Scheele, G. F. and Hanratty, T. J. 1962. Effect of natural convection on stability of flow in a vertical pipe. *J. Fluid Mech.* **14**, 244–256

Sparrow, E. M., Chrysler, G. M. and Azevedo, L. F. 1984. Observed flow reversals and measured-predicted Nusselt numbers for natural convection in a one-sided heated vertical channel. *ASME J. Heat Transfer.* **106**, 325–332

Van Doormaal, J. P. and Raithby, G. D. 1984. Enhancements of the SIMPLE method for predicting incompressible fluid flows. *Numer. Heat Transfer.* **7**, 147–163

Weast, R. C. and Lide, D. R. 1989. *CRC Handbook of Chemistry and Physics*, 70th ed, CRC Press, Boca Raton, FL